Crystal Structure of a Human Low Molecular Weight Phosphotyrosyl Phosphatase

IMPLICATIONS FOR SUBSTRATE SPECIFICITY*

Marie Zhang‡§, Cynthia V. Stauffacher¶, Dayin Lin‡, and Robert L. Van Etten‡‖

Departments of ‡Chemistry and ¶Biological Sciences, Purdue University, West Lafayette, Indiana 47907-1393

The low molecular weight phosphotyrosine phosphatases (PTPases) constitute a distinctive class of phosphotyrosine phosphatases that is widely distributed among vertebrate and invertebrate organisms. In vertebrates, two isoenzymes of these low molecular weight PTPases are commonly expressed. The two human isoenzymes, HCPTPA and HCPTPB, differ in an alternatively spliced sequence (residues 40–73) referred to as the variable loop, resulting in isoenzymes that have different substrate specificities and inhibitor/activator responses. We present here the x-ray crystallographic structure of a human low molecular weight PTPase solved by molecular replacement to 2.2 Å. The structure of human low molecular weight PTPase is compared with a structure representing the other isoenzyme in this PTPase class, in each case with a sulfonate inhibitor bound to the active site. Possible aromatic residue interactions with the phosphotyrosine substrate are proposed from an examination of the binding site of the inhibitors. Differences are observed in the variable loop region, which forms one wall and the floor of a long crevice leading from the active-site loop. A set of residues lying along this crevice (amino acids 49, 50, and 53) is suggested to be responsible for differences in substrate specificity in these two enzymes.

A wide variety of cellular processes are linked by cascades of phosphorylation and dephosphorylation of proteins, catalyzed by enzymes that set up subtly balanced molecular signals that regulate the rhythms of the cell. These enzymes encompass a large group of kinases and phosphatases that modify serine/threonine or tyrosine residues on other enzymes, receptors, transcription factors, and binding proteins. Several major groups of phosphotyrosine phosphatase (PTPase)[1] enzymes have been extensively studied. A high molecular weight PTPase family includes the receptor-like PTPases, such as CD45 and LAR, and nonreceptor PTPases, such as PTP1B and

Yersinia PTPase. The sequence identity within the 30-kDa catalytic domain of these enzymes is roughly 30–40%, in contrast to the presence of little apparent conservation in the remainder of the sequence, and suggests a highly conserved catalytic domain. Crystallographic studies of these PTPases as well as a so-called dual specificity enzyme showed that their catalytic domains indeed share a high degree of structure homology (1–5).

The low molecular weight PTPases are a distinctive class of soluble proteins with an M_r of approximately 18,000 (6, 7). These PTPases, which are highly conserved among themselves and have been identified and isolated from a wide variety of sources, exhibit no apparent sequence homology with the high molecular weight PTPases, with the exception of the PTPase signature sequence C*XXXXX*R(S/T) at the phosphate binding site (6). Surprisingly, although the crystallographic and solution structures of the bovine low molecular weight PTPase (8, 9, 10) revealed a new fold for a tyrosine phosphatase, they also revealed an active site that is virtually superimposable on that of the high molecular weight enzymes (6). A recent high resolution structure of a transition state analog complex of the bovine enzyme established that enhanced hydrogen bonding to the equatorial oxygens of the trigonal bipyramid occurs in the transition state, enforced by the relative rigidity of the phosphate binding loop (11). The similarities in the active sites of other PTPases suggests a highly similar catalytic mechanism.

In contrast to the mechanistic similarities, the substrate specificities of the various high and low molecular weight PTPases differ markedly. Moreover, even within a specific PTPase class, structural variations lead to the existence of isoenzymes that may exhibit different catalytic properties. Distinctive isoenzymes of the human low molecular weight tyrosine phosphatase have been identified (12–14). Based on protein and cDNA sequencing, activity studies, and mRNA blotting, it is now clear that the human enzyme known as erythrocyte acid phosphatase (E.C.3.1.3.2) is actually a PTPase and is present in all major human tissues (15–17). In human populations, this phosphatase exhibits stable polymorphisms and so has attained a major role as a forensic and genetic marker (18, 19). A large structural modification defines two major groups of isoenzymes, namely an alternative sequence segment corresponding to amino acid residues 40–73 in the mature human protein (13, 17) (Fig. 1). This segment, which we refer to as the variable loop, affects a number of physical and catalytic properties of the isoenzymes (22–24). It results from alternative mRNA splicing (17, 25, 26) and gives rise to the two major isoenzyme forms termed "fast" and "slow" on the basis of their electrophoretic mobility (15). In the human PTPases, the fast and slow electrophoretic forms correspond to the isoenzymes HCPTPA and HCPTPB (17). From their differences in behavior toward substrates and inhibitors, it appears possible that the two isoen-

[1] The abbreviations used are: PTPase, phosphotyrosine phosphatase; BPTP, bovine low molecular weight phosphotyrosine phosphatase; HCPTPA and HCPTPB, two isoenzymes of human low molecular weight phosphotyrosine phosphatase; MES, 4-morpholineethanesulfonic acid.

FIG. 1. **Sequence alignment of human (HCPTPA and HCPTPB) and bovine (BPTP) low molecular weight phosphotyrosyl phosphatases (17, 20).** Secondary structure elements shown under the sequences represent the structure of the human isoenzyme HCPTPA as established here. HCPTPA is the electrophoretically fast form of the isoenzyme, and HCPTPB is the slow form. BPTP is 94% identical in sequence to the human B (slow form) but only 81% identical to the human A (fast form) (17). Critical catalytic residues are *highlighted* in *black*. The universal PTPase consensus sequence C*XXXXX*R(S/T), which forms the active site P loop, appears in these proteins as the sequence CLGNICRS from residues 12 to 19 (*black highlighting*). The acidic residue Asp-129, which protonates the tyrosyl leaving group, is also *highlighted* in *black*. The variable sequence region that defines the difference between the human isoenzymes lies between residues 40 and 73 (*gray highlighting*). This figure was created with the program ALSCRIPT (21).
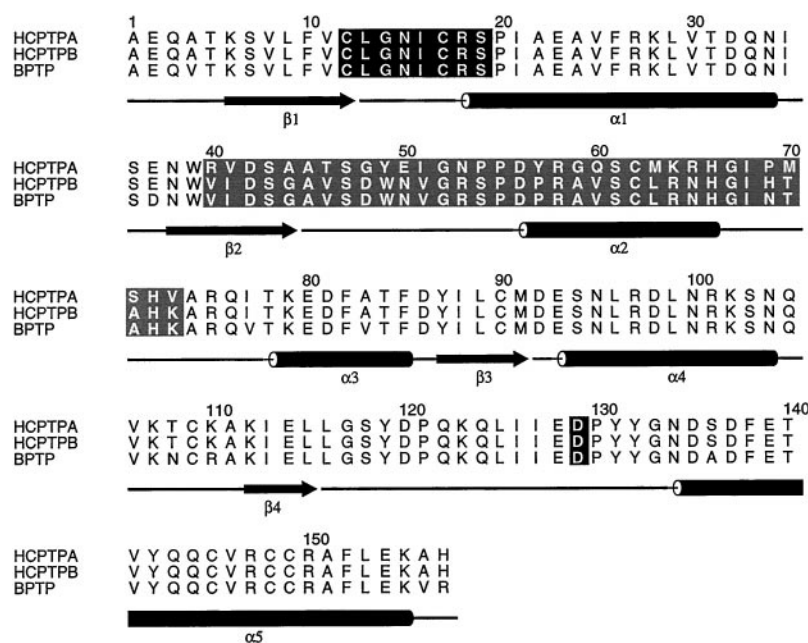
zymes may have different natural substrates and perform different physiological functions.

In addition to substrate specificity differences between these two isoenzymes, some residues that are conserved in the isoenzymes show different intrinsic properties. In the human isoenzyme HCPTPB and the bovine low molecular weight PTPase (BPTP), both His-66 and His-72 have unusually high pK_a values, 8.36 and 9.19, respectively (23). Based on the BPTP structure, it was proposed (8) that two acidic residues (Glu-23 and Asp-42) located near His-72 and an acidic residue (Glu-139) found near His-66 were primarily responsible for altering the pK_a values of the two histidine residues, and this has been confirmed in a detailed experimental and theoretical examination (27). In HCPTPA, His-72 also has an anomalously high pK_a of 9.23. In contrast, the pK_a of His-66 is 7.67, which is close to that of free histidine in solution despite the fact that Glu-139 is conserved in HCPTPA (23). Thus, the structural basis for this pK_a alteration of His-66 in HCPTPA was unknown.

To provide the basis for answering these and other questions related to the cellular role of this enzyme, we describe here the first three-dimensional structure of a human low molecular weight PTPase isoenzyme, HCPTPA (human red cell fast form) and compare this with the previously reported structure of BPTP (a protein that is expected to most closely resemble the human red cell slow electrophoretic form) (8–10). These enzymes have been solved in complex with the sulfonate inhibitors, MES, and HEPES, respectively.

EXPERIMENTAL PROCEDURES

HCPTPA was purified using a previously described procedure (17). Rod-shaped crystals (0.1 × 0.1 × 0.8 mm) were produced in hanging drops with a 10 mg/ml solution of HCPTPA, 30% polyethylene glycol monomethyl ether (M_r 5000), and 200 mM (NH$_4$)$_2$SO$_4$ in 100 mM MES buffer, pH 6.5 as the well solution, using microseeding techniques with crushed clusters of small spontaneous HCPTPA crystals grown under the same conditions. HCPTPA crystallized in the orthorhombic space group, P2$_1$2$_1$2$_1$, with unit-cell parameters of a = 34.1 Å, b = 56.6 Å, and c = 97.3 Å. Assuming 1 molecule/asymmetric unit, the calculated V_M is 2.61 Å^3/Da. The HCPTPA crystals diffracted to beyond 2.2 Å resolution and were stable for approximately 8 h in the beam. X-ray diffraction data from HCPTPA crystals were collected on a R-Axis IIC imaging plate system (Molecular Structure Corp.) mounted on a Rigaku RU200 rotating anode x-ray generator operating at 50 kV, 100 mA. Diffraction data were measured from two crystals with a 1.0° oscillation angle and 120-mm crystal detector distance. All data were indexed and integrated using the program Denzo and merged and scaled together with the program Scalepack (28).

The initial structure determination was done with data to 2.2 Å taken from a single crystal (80% complete). Rotation and translation function searches were performed with these data in the program AMoRe (29) using as the model the complete bovine heart PTPase structure (8). An 8.0–2.3 Å cross-rotation function search with a radius of integration of 20 Å and an angular step size of 1.5° produced a unique solution at α = 147.94°, β = 81.81°, and γ = 207.31°. The Crowther and Blow translation function identified the optimal translation at x = 0.07706, y = 0.09339, and z = 0.12038. The R-factor calculated from AMoRe after rigid-body refinement was 37.6%. This rotation function solution was used to produce an electron density map for HCPTPA at 2.2 Å into which a model was built. After three rounds of rebuilding in 2Fo-Fc maps and omit 2Fo-Fc maps, the model was put into refinement in XPLOR (30) with an initial R-factor of 33.5% for data from 20 to 2.8 Å (35.8% for data to 2.2 Å). The model was refined using simulated annealing followed by positional refinement and cycles of refitting. With individual B-factors, the refinement converged to an R-factor to 2.8 Å of 20.0% with an R-free of 32.2% for 355 reflections (9% total measured reflections). The reflection data to 2.2 Å were then included in the refinement, and a similar protocol followed with the addition of 82 water molecules (R-factor of 18.6% and R-free of 25.4%). A MES molecule was found in this improved map, bound to the active site, and built into the density. At this stage, additional data were taken from a second large crystal, resulting in a 2.2 Å data set that was 92% complete. Refinement in XPLOR using the data to 2.2 Å was repeated starting with the unrefined HCPTPA model. The resulting structure showed only minor changes from the previously refined model, although the density maps were significantly improved. The final refined model of HCPTPA consisted of 157 amino acids, 82 water molecules, and 1 MES molecule and had an R-factor of 18.1% and R-free of 24.8%. The first four amino acids at the N terminus and the last two amino acids at the C terminus have poor electron density. The final refined model possessed good geometry with r.m.s. deviations of bond length of 0.015 Å and bond angle of 2.018°. The average temperature factor for the protein (residues 5 to 157) is 22.9 Å^2 for the main chain and 27.0 Å^2 for side chains. The Ramachandran plot showed no outliers and demonstrated that more than 90% of the residues were in the most favored regions. Data collection and refinement statistics are summarized in Table I.

RESULTS AND DISCUSSION

The overall topology of the human low molecular weight PTPase isoenzyme A (Fig. 2) closely resembles that of the bovine enzyme (r.m.s. deviation of C$_\alpha$s is 0.42 Å). Like the structure of BPTP, the structure of HCPTPA consists of a four-stranded central parallel β sheet with flanking α helices

Human Low Molecular Weight PTPase Structure

TABLE I
Diffraction data and refinement statistics for the HCPTPA structure determination

Crystal parameters	
Space group	$P2_12_12_1$
a (Å)	34.1
b (Å)	56.6
c (Å)	97.3
Z (mol/asymetric unit)	1
Data processing statistics	
Resolution (Å)	40 to 2.2 Å
Crystal (*n*)	2
Measurements (*n*)	102917
Unique reflections (*n*)	9356
% Complete	92.2
Rsym[a] (%)	0.077
Refinement statistics	
Reflections (*n*)	8525
Protein and ligand atoms (*n*)	1564
Water molecules (*n*)	82
R-factor[a] (%)	18.1
R-free (%)	24.8
r.m.s. bond lengths (Å)	0.015
r.m.s. bond angles (degrees)	2.018

[a] Rsym = $\Sigma \mid (I_{hkl} - I_{hkl}) \mid / \Sigma I_{hkl}$, where I_{hkl} is the average of I_{hkl} over all symmetry equivalents. R-factor = $\Sigma \mid Fo - Fc \mid / \Sigma Fo$ where Fo and Fc are the observed and calculated structure factors.

on both sides, showing two right-handed $\beta\alpha\beta$ motifs. The active site of HCPTPA is located at the C-terminal end of $\beta1$ of the central, parallel β sheet and at the N terminus of the first α helix ($\alpha1$). The consensus PTPase sequence motif C*XXXXX*R(S/T), which is present as the sequence CLGNICRS in HCPTPA, forms a loop connecting the first β strand and the first turn of the helix $\alpha1$ in the structure (Fig. 2). HCPTPA does not contain the typical glycine-rich P-loop or Walker-A sequence motif associated with nucleotide-binding proteins (31), but the active site sequence folds into a peptide backbone arrangement that is identical to that of a P-loop structure (8, 32). In the crystal of HCPTPA, a MES molecule was found at the active site, with its sulfonate moiety sitting in the phosphate binding pocket. Three oxygens on the sulfonate group form multiple hydrogen bonds with the NHs on the backbone of the active site loop as well as the nitrogens of the side chain of the conserved Arg-18 in a fashion similar to that of the phosphate bound in the active site of the original BPTP structure (8). The BPTP structure complexed with a similar sulfonate derivative, HEPES, was also solved using difference Fourier techniques (11). Both MES and HEPES molecules were found to be well ordered in the structures with average temperature factors of 29.3 Å^2 and 39.3 Å^2, respectively, as shown by the electron density of the MES and HEPES molecules (Fig. 3). The sulfonate moiety in both MES and HEPES showed even lower average temperature factors, 22.9 Å^2 in MES and 18.8 Å^2 in HEPES, which is very close to the average temperature factor of the backbone of the active site. Although the active site loops of HCPTPA and BPTP are virtually superimposable, the relative positions of the structure of MES and HEPES at the active site are not identical (Fig. 4). In both cases, the sulfonate moiety sits in the center of the active site loop, but the orientation of the six-membered rings differ by a 60 degree relative rotation. However, because the MES molecule is located in one of the intermolecular contact sites in the crystal, the position of the MES molecule could be strongly influenced by crystallographic packing and may not represent its natural position in solution.

Close examination of the surrounding residues near His-66 in the structure of HCPTPA also provided the explanation of why His-66 has a relatively normal pK_a of 7.67, compared with
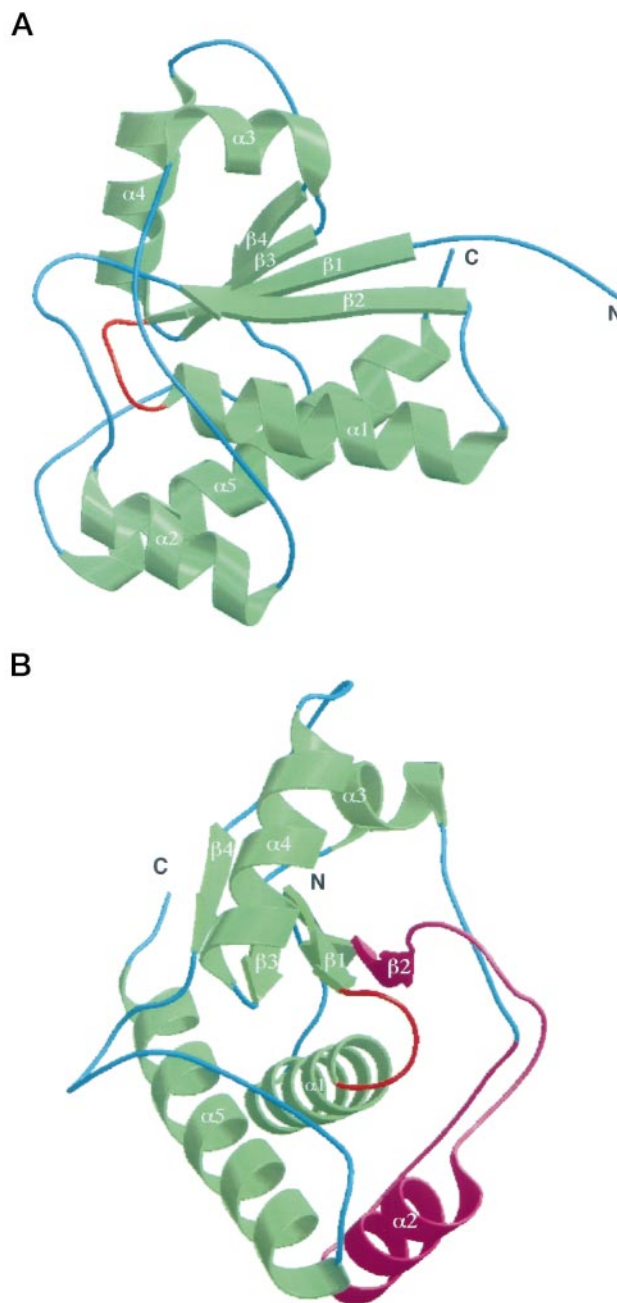

FIG. 2. **Ribbon diagrams of the fold of human low molecular weight tyrosine phosphatase (HCPTPA).** Two views of the molecule are shown in *A* and *B*, separated by a 90° rotation around the vertical axis. The active-site sequence CLGNICRS forms a loop connecting the first β strand ($\beta1$) to the first turn of the helix, $\alpha1$. The variable sequence in the two isoenzymes exists as a segment that contains most of $\beta2$, the loop connecting $\beta2$ and $\alpha2$, the helix $\alpha2$, and part of the loop after $\alpha2$ (*highlighted* in *purple* in view *B*). This portion of the structure wraps around the active-site loop and is proposed to be important for the substrate specificity of the two isoenzymes.

that of His-66 in BPTP, which is 8.36. In BPTP, an acidic residue (Glu-139) was found near His-66 and therefore was proposed to be responsible for the altered pK_a (8, 27). Although Glu-139 is conserved between the two enzymes, the amino acids that surround this residue in the three-dimensional structure are clearly different. In the HCPTPA structure, an arginine (Arg-65) appears to interact with Glu-139. In the BPTP structure, residue 65 is an asparagine and is too distant to interact with Glu-139. It is likely that the negative charge on Glu-139 is shared between His-66 and Arg-65, resulting in a relatively normal pK_a for His-66.
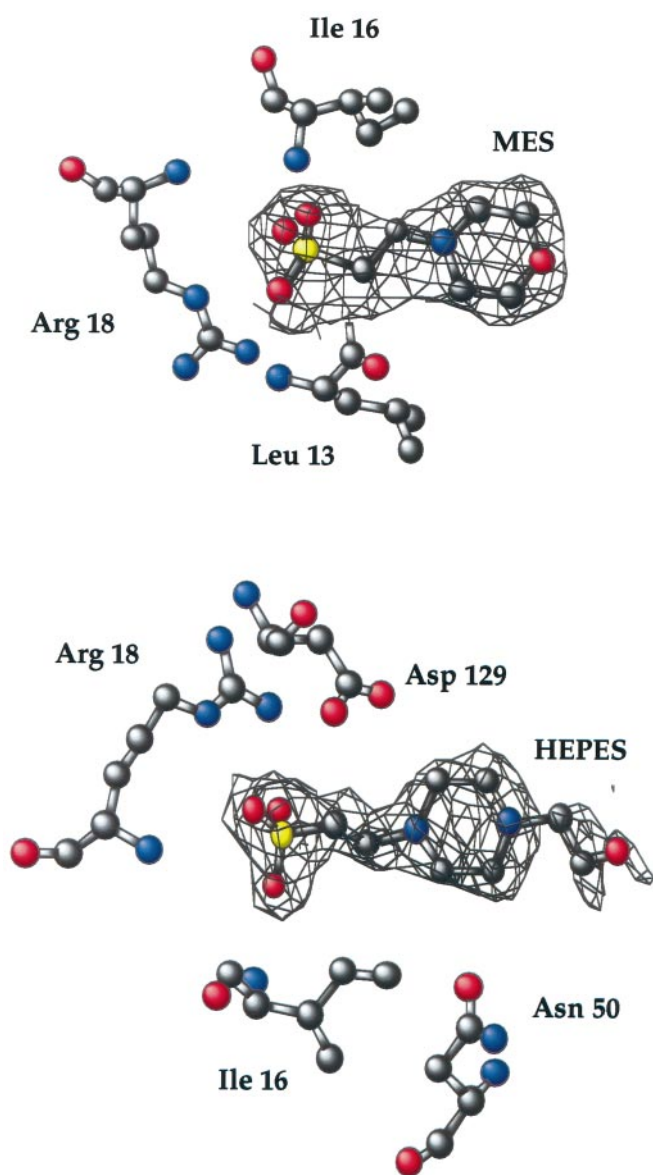
FIG. 3. **2Fo-Fc electron density for MES and HEPES in the structures of HCPTPA and BPTP.** In each case the view shown is perpendicular to the inhibitor ring. Residues immediately surrounding these sulfonate inhibitors are shown, including the Arg-18 of the active-site loop. The density for the inhibitors is contoured at a level corresponding to that of the protein (1.5σ) and indicates that both molecules are well-ordered in the structure.

Biochemical studies have shown that the isoenzyme class containing HCPTPB and BPTP often behaves very differently toward substrates than does the HCPTPA isoenzyme. This includes not only reactivity to small synthetic substrates but also toward more physiological protein targets. For example, HCPTPA exhibited a much higher activity, as compared with HCPTPB and BPTP, toward phosphotyrosyl angiotensin II, RR-src, and myelin basic protein (Table II). An examination of the surface structure and charge distribution indicates a structural source for some of the differences between the isoenzymes and their binding of the substrates and inhibitors. Effectively, all of the amino acid variations of the two isoenzymes occur on one side of the molecule (to the right in Figs. 2*B* and 5*A*), indicating that this portion of the PTPase structure could be an important site for the interaction between the enzyme and its physiological substrate or other biological targets. One of the most striking features of the low molecular weight PTPase
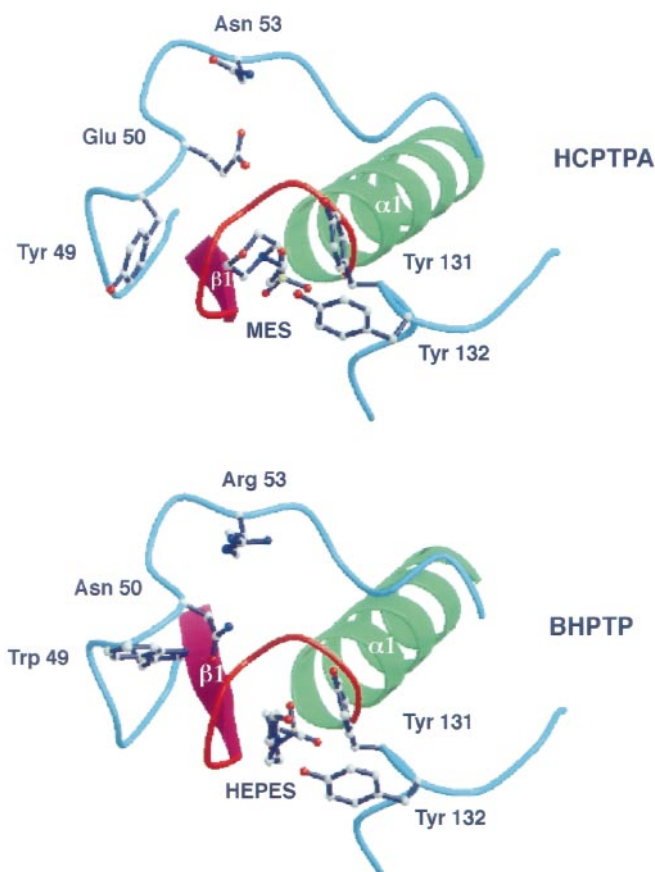

FIG. 4. **The active sites of the structures of HCPTPA and BPTP in complex with sulfonate inhibitors.** Shown here are the active-site loop (in *red*), a portion of the variable loop containing residues 50 and 53, one of the aromatic claws (residue 49), and a portion of the loop between $\beta4$ and $\alpha5$, which contains the other two aromatics (Tyr-131 and -132). The overall backbone arrangement at the active site and the positions of 131,132 are identical for the two isoenzymes. In the HCPTPA structure, Tyr-49 forms an interaction with the inhibitor, MES, stacking face to edge with the morpholino ring, whereas in the BPTP structure, Trp-49 does not appear to interact with the bound inhibitor, HEPES. The residues, 50 and 53, located on the variable loop bordering the active site, also change in nature, altering the charge surface on one wall of the crevice near the active site from negative in HCPTPA (Glu-50/Asn-53) to positive in BPTP (Asn-50/Arg-53).

TABLE II
Specific activity (units/mg) of low molecular weight tyrosine phosphatases toward phosphorylated peptides and proteins (24)

Substrate	Enzyme		
	HCPTPA	HCPTPB	BPTP
p-Nitrophenyl phosphate	53	95	100
Val[5] angiotensin II[a] (DRVpYVHPF)	345	183	177
RR-src[a] (RRLIEDAEpYAARG)	375	24	55
Myelin basic protein[b]	343	138	158

[a] The data were determined by using a P81 phosphocellulose filter assay.

[b] The data were determined by using activated charcoal extraction methods.

structures in this region is a shallow crevice leading from one side of the molecule into the active site (Fig. 5*A*). The variable loop, which determines the isoenzyme type, forms one wall and the floor of this crevice, whereas the loop between $\beta4$ and $\alpha5$, which contains the catalytically critical Asp-129 (33), forms the other wall. A set of three aromatic residues (Tyr-49, Tyr-131, Tyr-132) reaches out like claws from either wall near the active site. The structure of the variable loop in this region is quite rigidly determined by a proline-proline sequence in the crevice
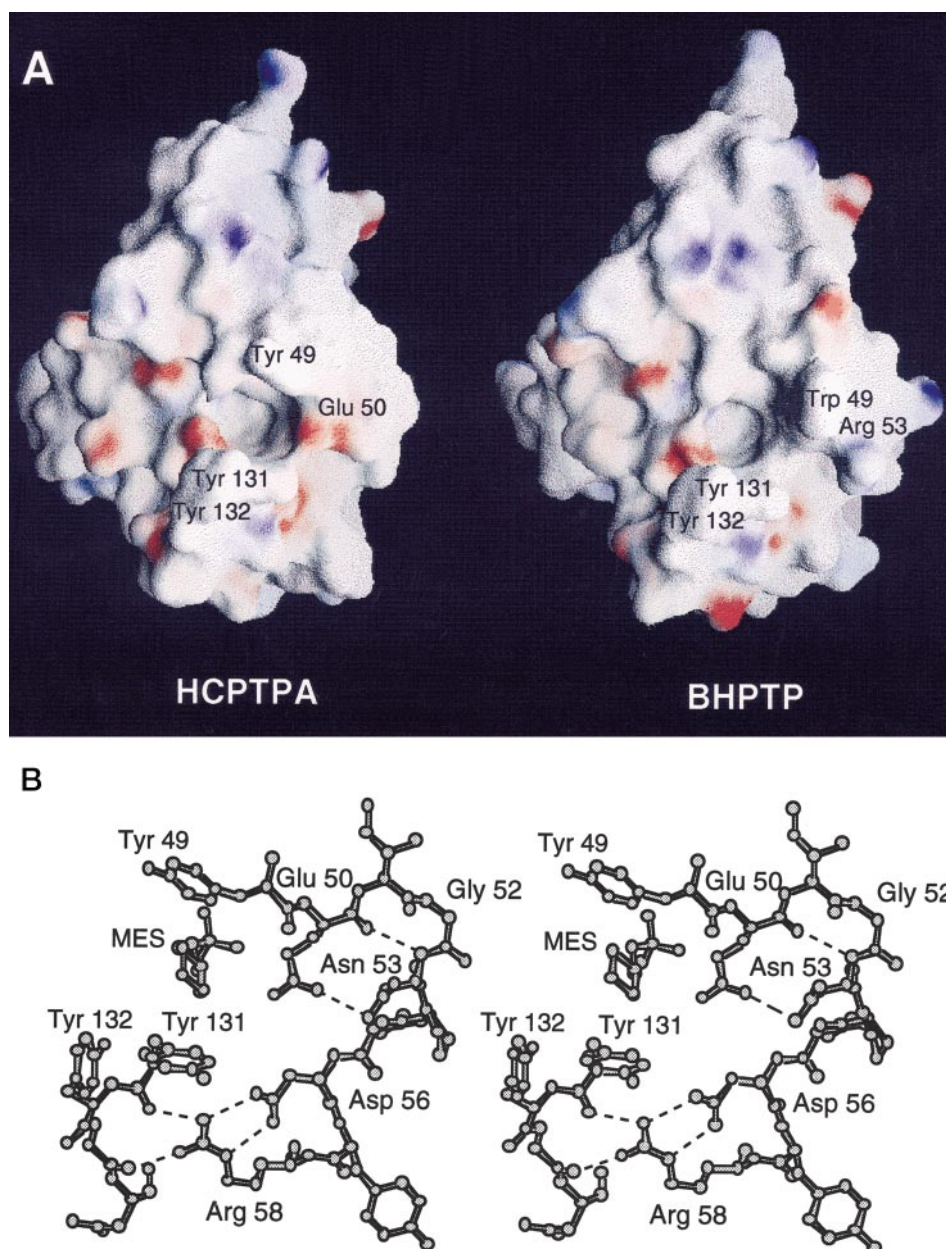
FIG. 5. *A*, a smoothed surface and charge distribution representation of HCPTPA and BPTP viewed directly into the active site, which appears as a circular depression at the center of the molecule. (This view of the molecule corresponds roughly to view *B* shown in Fig. 2.) The crevice leading into the active-site pocket from the lower right is proposed to be the peptide binding site. Charge distributions are indicated by *red* (negative) and *blue* (positive). The most dramatic charge alteration on the surface is near the active site, due to changes in residues 50 and 53, which border the crevice. *B*, stereo diagram showing the construction of the crevice and aromatic claws from variable loop residues 49 to 58 and the $\beta4-\alpha5$ loop that contains residues 131 to 134 in HCPTPA. Residues 50 to 53 form a type II β turn, positioning Glu-50 and Asn-53 on one wall of the crevice. Residues 56 and 58 form a salt bridge, and residue 58 interacts with two carbonyl oxygens of the backbone of the loop that contains residues Tyr-131 and -132, positioning them on the opposite wall.

floor of HCPTPA, together with a set of hydrogen bonds that align the residues along the crevice walls (Fig. 5B). A β kink with a type II hydrogen bond in the variable loop positions residues 50 and 53 pointing toward the crevice and places the aromatic residue at 49 into a position above the active site. Toward the C-terminal end of this structure, two of the conserved residues in the variable loop, Asp-56 and Arg-58, form a set of hydrogen bonds with the backbone of the $\beta4$-$\alpha5$ loop. This interaction positions the aromatic claws of Tyr-131 and -132 on the opposite side of the active site, forming a hydrophobic wall against which the phosphorylated tyrosine ring of the substrate would be expected to lie.

The differences between the HCPTPA and BPTP structures in these regions suggests residues critical for substrate

recognition. The variable loop residue 49, which is Tyr in HCPTPA and Trp in BPTP (and HCPTP), forms one of the aromatic claws located above the active site. Differences in the positions of these two residues appear to parallel the differences in the ring position of the bound sulfonate inhibitor (Fig. 4). In the BPTP complex, the side chain of Trp-49 extends away from the active site and does not appear to interact with HEPES molecule. In contrast, in the HCPTPA complex, the side chain of Tyr-49 flips back into the active-site pocket and stacks face to edge with the morpholino ring of the MES molecule. This holds the ring of the MES molecule in the active site, sandwiched between Tyr-49 on one side and Tyr-131 and Tyr-132 on the other. The position of the two aromatic residues on the opposite side of the active site is

identical in both structures, with edge-to-face interactions between all three rings. We believe that the hydrophobic sandwich seen in these low molecular weight PTPase structures may reflect the binding of the ring portion of the natural phosphotyrosine substrate. It has also been reported that Tyr-131 and -132 can be transiently phosphorylated and can themselves serve as substrates for a second molecule of phosphatase (34), suggesting a possible control mechanism associated with these active-site residues.

An examination of the variable loop portions of the wall of the crevice that leads to the aromatic claws at the active site of the two structures shows that there is a dramatically different charge pattern that is the result of changes in residues 50 and 53 (Fig. 5*A*). Changes of Glu to Asn at residue 50 and Asn to Arg at residue 53 (in HCPTPA and in BPTP, respectively) result in a change from a negative patch near the active site of HCPTPA to a positive patch in BPTP, a difference that occurs between all fast and slow isoenzyme forms. This distinct charge alteration near the active site would be expected to cause the two isoenzymes to recognize amino acids with different charges as part of potential peptide or protein substrates. To test this, we measured the specificity constants k_{cat}/K_m for two phosphotyrosyl peptides that possess differing charge complementarities. Hydrolysis of a predominantly negatively charged molecule, the epidermal growth factor-related phosphopeptide SLDNPDpYQQDFF, by HCPTPA and -B gave nearly identical k_{cat}/K_m values of 88 and 83 $M^{-1} s^{-1}$, respectively. In contrast, hydrolysis of a predominantly positively charged peptide, the STAT-related peptide QERRKpYLKHRLIVV by HCPTPA and -B gave k_{cat}/K_m values of 95 and 18 $M^{-1} s^{-1}$, respectively. These results demonstrate that multiple positive charges surrounding the phosphotyrosine in a peptide tends to disfavor its hydrolysis by the B-type isoenzyme.[2] Given their position facing into the crevice in close proximity to the site where the phosphotyrosine binds, it appears that two residues, 50 and 53, are the critical determinants of a specific charge distribution recognition that is important in determining the natural substrates of these isoenzymes. Evidence that the residue at position 50 is important for selectivity has been presented by Cirri *et al.* (35), based on studies done with the rat low molecular weight PTPases. Preliminary results from a more extensive study of the human enzyme properties in our laboratory using both chemical and biological substrates and inhibitors show that in fact all three variable loop residues (positions 49, 50, and 53) have significant roles in determining the specificities of the two enzymes.[3]

Similar features that contribute to substrate binding and specificity also occur in the high molecular weight PTPases. For example, the aromatic residues near the active site, which provide a hydrophobic surface for interacting with the ring of the phosphorylated tyrosine, can be seen in all PTPase structures. Where the HCPTPA structure shows a set of aromatic claws on both sides, the high molecular weight PTPases appear to have a single aromatic residue. The single conserved aromatic residue near the active site in these high molecular weight PTPases (Tyr-46 in PTP1B and Phe-229 in *Yersinia* PTPase) occupies a similar position as Tyr-49 in HCPTPA or Trp 49 in BPTP and was originally thought to confer stabilization in binding for the Tyr(P) (1, 2). However, in the structure of PTP1B complexed with a phosphorylated peptide, another aromatic residue (Phe-182) is found near the active site in a similar position as Tyr-131, situated on a loop that moves toward the substrate in the complex (36). The

phenylalanine (Phe-182) side chain provides a site for a hydrophobic interaction with the aromatic ring of pTyr in the bound peptide. This loop movement is also seen in the *Yersinia* PTPase structures with nitrate, vanadate, and tungstate (37). Interactions of *Yersinia* phosphotyrosine phosphatase with a phosphorylated tyrosine have been modeled on the structures of these complexes in which the loop movement brings a glutamine (Gln-46) into the analogous Tyr-131 site (38).

The members of the low molecular weight PTPase family were proposed to have similar three-dimensional structures because of their high sequence homology (8). Indeed, we have shown that the overall structure of HCPTPA appears quite similar to that of BPTP. However, although the two enzymes possess the same three-dimensional fold, they may have distinctly different physiological functions as a consequence of side chain differences near the active site mediated by the charges in the variable loop residues. Finally, there is a developing body of evidence that the human low molecular weight PTPase plays a role in the engagement and activation of ELK and Nuk signaling complexes that accompanies capillary-like endothelial assembly (39, 40). Ultimately, the interpretation of such phenomena at the molecular level will require structural data such as that presented here.

REFERENCES

1. Stuckey, J. A., Schubert, H. L., Fauman, E. B., Zhang, Z.-Y., Dixon, J. E., and Saper, M. A. (1994) *Nature* **370,** 571–575
2. Barford, D., Flint, A. J., and Tonks, N. K. (1994) *Science* **263,** 1397–1404
3. Bilwes, A. M., den Hertog, J., Hunter, T., and Noel, J. P. (1996) *Nature* **382,** 555–559
4. Hoffmann, K. M. V., Tonks, N. K., and Barford, D. (1997) *J. Biol. Chem.* **272,** 27505–27508
5. Yuvaniyama, J., Denu, J. M., Dixon, J. E., and Saper, M. A. (1996) *Science* **272,** 1328–1331
6. Zhang, M., Stauffacher, C. V., and Van Etten, R. L. (1995) *Advances in Protein Phosphatases* (Merlevede, W., ed) Vol. 9, pp. 1–23, Leuven University Press, Leuven, Belgium
7. Ramponi, G. (1994) *Advances in Protein Phosphatases* (Merlevede, W., ed) Vol. 8, pp. 1–25, Leuven University Press, Leuven, Belgium
8. Zhang, M., Van Etten, R. L., and Stauffacher, C. V. (1994) *Biochemistry* **33,** 11097–11105
9. Su, X.-D. Taddei, N., Stefani, M., Ramponi, G., and Nordlund, P. (1994) *Nature* **370,** 575–578
10. Logan, T. M., Zhou, M.-M., Nettesheim, D. G., Meadows, R. P., Van Etten, R. L., and Fesik, S. W. (1994) *Biochemistry* **33,** 11087–11096
11. Zhang, M., Zhou, M., Van Etten, R. L., and Stauffacher, C. V. (1997) *Biochemistry* **36,** 15–23
12. Yoshihara, C. M., and Mohrenweiser, H. W. (1980) *Am. J. Hum. Genet.* **32,** 898–907
13. Dissing, J., Johnsen, A., and Sensabaugh, G. F. (1991) *J. Biol. Chem.* **266,** 20619–20625
14. Dissing, J., and Johnsen, A. H. (1992) *Biochim. Biophys. Acta* **1121,** 261–268
15. Hopkinson, D. A., Spencer, N., and Harris, H. (1963) *Nature* **199,** 969–975
16. Waheed, A., Laidler, P. M., Wo, Y.-Y. P., and Van Etten, R. L. (1988) *Biochemistry* **27,** 4265–4273
17. Wo, Y.-Y. P., McCormack, A. L., Shabanowitz, J., Hunt, D. F., Davis, J. P., Mitchell, G. L., and Van Etten, R. L. (1992) *J. Biol. Chem.* **267,** 10856–10865
18. Cavalli-Sforza, L., Menozzi, P., and Piazza, A. (1994) *The History and Geography of Human Genes*, pp. 185–186, 246, 288, 367, 369; map pages 6, 7, and 118–127, Princeton University Press, Princeton, NJ
19. Sokal, R. R., Oden, N. L., and Wilson. C. (1991) *Nature* **351,** 143–145
20. Wo, Y.-Y. P., Zhou, M.-M., Stevis, P., Davis, J. P., Zhang, Z.-Y., and Van Etten, R. L. (1992) *Biochemistry* **31,** 1712–1721
21. Barton, G. J. (1993) *Protein Eng.* **6,** 37–40
22. Dissing, J., Rangaard, B., and Christensen, U. (1993) *Biochim. Biophys. Acta* **1162,** 275–282
23. Zhou, M.-M., Davis, J. P., and Van Etten, R. L. (1993) *Biochemistry* **32,** 8479–8486
24. Wo, W.-Y. P. (1992) *Cloning, Expression, and Characterization of Low Molecular Weight Acid Phosphatases from Bovine Heart and Human Placenta*, Ph.D. thesis, Purdue University
25. Lazaruk, K. A., Dissing, J., and Sensabaugh, G. F. (1993) *Biochem. Biophys. Res. Commun.* **196,** 440–446
26. Bryson, G. M., Massa, H., Trask, B. J., and Van Etten, R. L. (1995) *Genomics.* **30,** 133–140
27. Tishmack, P. A., Bashford, D., Harms, E., and Van Etten, R. L. (1997) *Bio-*

---

[2] A. D. Schroff, unpublished results.
[3] B. Evans, unpublished results.

    chemistry **36,** 11984–11994
28. Otwinowski, A. (1993) *Data Collection and Processing*, pp. 56–62, Daresbury Laboratory, Warrington, United Kingdom
29. Navaza, J. (1987) *Acta Crystallogr. Sec. A.* **43,** 645–653
30. Brunger, A. T., Kuriyan, J., and Karplus, M. (1987) *Science* **235,** 458–460
31. Schulz, G. G. (1992) *Curr. Opin. Struct. Biol.* **2,** 61–67
32. Evans, B., Tishmack, P. A., Pokalsky, C., Zhang, M., and Van Etten, R. L. (1996) *Biochemistry* **35,** 13609–13617
33. Zhang, Z., Harms, E., and Van Etten, R. L. (1994) *J. Biol. Chem.* **269,** 25947–25950
34. Tailor, P., Gilman, J., Williams, S., Couture, C., and Mustelin, T. (1997) *J. Biol. Chem.* **272,** 5371–5374
35. Cirri, P., Fiaschi, T., Chiarugi, P., Camici, G., Manao, G., Raugei, G., and

    Ramponi, G. (1996) *J. Biol. Chem.* **271,** 2604–2607
36. Jia, Z., Barford, D., Flint, A. J., and Tonks, N. K. (1995) *Science* **268,** 1754–1758
37. Schubert, H. L., Fauman, E. B., Stuckey, J. A., Dixon, J. E., and Saper, M. A. (1995) *Protein Sci.* **4,** 1904–1913
38. Fauman, E. B., Yuvaniyama, C., Schubert, H. L., Stuckey, J. A., and Saper, M. A. (1996) *J. Biol. Chem.* **271,** 18780–18788
39. Stein, E., Cerretti, D. P., Schoecklmann, H. O., Schroff, A. D., Van Etten, R. L., and Daniel, T. O. (1997) *ASBMB Satellite Meeting, Seattle, WA Aug. 20–23*, Abst. P5B-14
40. Stein, E., Lane, A. A., Cerretti, D. P., Schoecklmann, H. O., Schroff, A. D., Van Etten, R. L., and Daniel, T. O. (1998) *Genes Dev.* **12,** 667–678